Nanoengineering with dynamic atomic force microscopy: Lateral interchange of adatoms on a Ge(111)-$c(2\times8)$ surface

Peter Dieška[1] and Ivan Štich[2,*]

[1]*Center for Computational Materials Science (CCMS), Slovak University of Technology (FEI STU), Ilkovičova 3, SK-81219 Bratislava, Slovakia*

[2]*Institute of Physics, Slovak Academy of Sciences, SK-84511 Bratislava, Slovakia*

(Received 23 January 2009; published 25 March 2009)

Ab initio techniques are used to elucidate the lateral noncontact AFM pair exchange of Sn and Ge adatoms on the Ge(111)-$c(2\times8)$ surface both at low and room temperatures. Two different processes are considered: (a) tip-assisted surface diffusion and (b) active tip participation via adatom pick-up/deposition processes. The adatom diffusion profiles indicate fairly modest energy barriers between 0.6 and 0.8 eV, which can be further significantly reduced by the tip. However, the diffusion-mediated exchange mechanism is precluded by a large barrier (>1 eV) to the (Sn, Ge)-pair exchange. The experimental data are only consistent with a mechanism involving a simultaneous adatom pick-up/deposition and adatom diffusion processes. Simulation results show that, contrary to general belief, the tip apex modification due to the pick-up/deposition processes may not be experimentally noticeable.

DOI: 10.1103/PhysRevB.79.125431 PACS number(s): 81.16.Ta, 68.37.Ps, 71.15.Nc, 71.15.Pd

Noncontact/nearcontact atomic force microscope (NC AFM) (Refs. 1–3) has in the last decade demonstrated three unique capabilities: atomic resolution,[1–3] chemical resolution,[4,5] and nanomanipulation[6–8] for both semiconducting/insulating and conducting materials. While a lot of progress has been seen in understanding atomic-scale image formation[9–12] and to a lesser degree also in chemical resolution,[5] the nanomanipulation, subject of the present study, is less well understood when it comes to comprehending the atomic-scale processes.[13–15]

Lateral manipulation of single atoms and molecules has long been seen as the cornerstone of two-dimensional nanoengineering. Scanning tunnel microscope (STM), and more recently NC AFM, has provided the capabilities to perform well-controlled manipulation of components strongly bonded to the surfaces, such as atoms or molecules. Nanomanipulation was long pioneered by STM. Vertical and lateral manipulations of individual atoms,[16] molecules,[17] and bonds[18] have been demonstrated. Only much later was, for the first time, NC AFM used for vertical manipulation of adatoms on the Si(111)-7×7 surface in constant excitation mode.[6] Soon lateral manipulation of individual atoms followed. Oyabu *et al.*[7] succeeded in laterally moving a single Ge adatom on Ge(111)-$c(2\times8)$ surface. Later they reported an interchange manipulation of Sn and Ge atoms on the same surface[8] with part of Ge adatoms substituted by Sn in constant frequency shift mode. Despite the fact that all reported atomic manipulations are experimentally well reproducible, their mechanisms are only gradually uncovered. The same is true of most of the STM manipulations, where too atomic/molecular-scale understanding of experimental protocols is still often missing. In this respect simulation techniques have proven extremely useful in providing insights into the vertical atomic manipulation.[19] The purpose of the present paper is to shed light on the lateral manipulation. This is obviously a very general question, which can only be addressed in a meaningful way by analyzing the mechanisms of experimentally well-controlled specific representative systems. For example, understanding of lateral manipulation of adatoms on Si(111)-7×7 surface was recently provided.[20] Here we study the (Sn, Ge)-pair exchange on the Ge(111)-$c(2\times8)$ surface.[8,21]

The Sn↔Ge interchange manipulation on the Ge(111)-$c(2\times8)$ surface is unique as the Sn and Ge adatoms could not only be moved in several different directions[8] (see Fig. 1) but also both at room[8] and low temperatures.[22] The experimental temperature range of 80–300 K indicates that the manipulation process is either not thermally activated or that under the action of the tip the diffusion barriers are

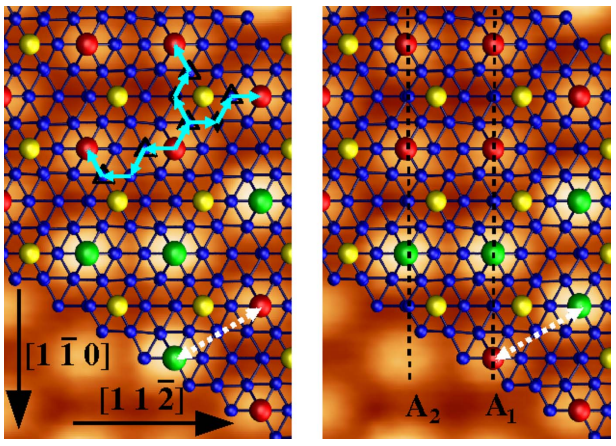

FIG. 1. (Color online) The experimental NC AFM image (Ref. 8) with superimposed ball-and-stick model before (left) and after (right) the (Sn, Ge)-pair exchange, see white arrows. Sn adatoms (green color) are imaged as brighter spots, and germanium adatoms are imaged as darker spots (red color). Rest atoms are shown in yellow. The two types of adatoms (A_1,A_2) are indicated by black dashed lines. The calculated lowest-energy pathways for adatom diffusion (Ref. 21) along the directions where manipulation was observed experimentally (Ref. 8) are shown by blue arrows, △ labels H_3 sites, and ◆ labels the midpoint site between two neighboring T_4 sites.

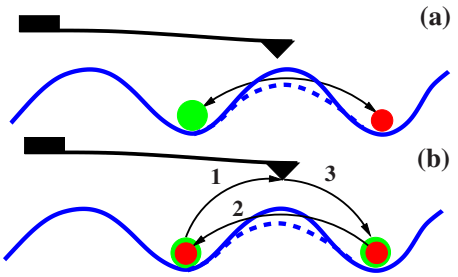

FIG. 2. (Color online) Schematics of the lateral manipulation processes. (a) indirect and (b) direct processes. The arrows (numbers) indicate the respective motions of the atoms during the exchange process. Color coding of atoms follows Fig. 1.

flattened and become vanishingly small. Two scenarios can be envisioned, see Fig. 2: (a) "indirect" process, where the tip is acting merely as a "catalyst" lowering the energy barriers for diffusion of the adatoms and (b) "direct" process with the tip actively participating in the exchange process, e.g., by adatom pick-up/deposition processes. Both scenarios are hard to reconcile with common sense and experimental evidence. While it is difficult to imagine a tip process leading to a local flattening of the potential-energy surface (PES) in different directions, as assumed in process (a), the pick-up/deposition processes (b) is expected to lead to signal (frequency shift) discontinuities in the manipulation process, which were not observed.[23] These conceptual problems cannot be addressed solely by experimental means, as experimental time scales [$O(10^5)$ Hz] are too slow to capture the dynamics of the manipulation processes.

Ideally, the manipulation process should be described by a complete simulation of the experimental NC AFM apparatus, including cantilever dynamics, effects of electronics, etc.[24] This, though, would require the knowledge of a complete PES for the manipulation process, in addition to the details of the experimental tip, its apex termination, elastic properties, etc. Such a wealth of detailed knowledge is unrealistic. For that reason we limit ourselves to just a number of PES calculations for very simple model systems which provide insights into the possible basic steps of the manipulation process.

The PESs were described at the density-functional theory level.[25] The electronic structure was modeled in plane-wave pseudopotential[26] formulation using the CPMD suite of codes.[25] All calculations were carried out using the Perdew-Burke-Ernzerhof functional,[27] Γ-point sampling of the surface Brillouin zone, and a 10 Ry plane-wave cutoff; see also Ref. 21. This basis set is sufficient in converging energy differences such as barrier heights. Increasing the plane-wave cutoff to 40 Ry changes the barrier heights by less than chemical accuracy. The surface was described by a slab model, three double-layer thick, doubling the unit-cell size in the short side direction, i.e., by a 4×8 surface unit cell with dangling bonds on the bottom layer of germanium atoms saturated by hydrogen atoms. The bottom layer and hydrogen saturation are kept fixed. The 4×8 surface unit cell is large enough to provide a fair sampling of the Brillouin zone by the Γ point for a semiconducting system. The dangling bonds in the bottom layer of the slab were saturated by hydrogen. Simple and well-tested model tips were used, a 10 atom germanium tip saturated at the base by hydrogen[9] and a dimer-terminated tip.[28] In addition, we use also a trimer-terminated tip, see below. In all tip models the germanium atoms in the tip base and the hydrogen termination were kept fixed. Static PESs were computed by both nudged elastic band (NEB) method[29] and by application of constraints. In practice, NBE was finding diffusion pathways along the $[1\bar{1}0]$ and $[11\bar{2}]$ directions, similarly to the method of constraints which, however, turned out to be computationally faster. Hence, most of the simulations were done by application of constraints. The simulation typically consists of moving the adatom (Sn or Ge) or simultaneously the (Sn, Ge)-pair on the surface in small steps with just one coordinate fixed, with or without presence of a tip, which itself may be moved in the direction normal to the surface. At each adatom/pair/tip position all ionic degrees of freedom are optimized, except for those kept fixed by the applied constraints. We noticed that the PESs exhibited hysteretic behavior and the PESs for forward and backward motions were not identical.[21] Further analysis revealed that the PESs consist of extremely flat terraces especially in the direction perpendicular to the surface. First-order optimization methods, such as conjugate gradients, left the structures "hanging" on the terraces causing the hysteresis. The same problem applies equally to the NEB method. For that reason we have reoptimized the structures typically by moving the Sn (Ge) adatom(s) in a wide range of distances toward the surface. Using the minima from the vertical scans resulted in totally symmetric PES without any hysteresis. Short molecular dynamics (MD) runs[25] were also performed.

Both proposed mechanisms (see Fig. 2) share one common feature, namely, the adatom destabilization from their T_4 positions by the tip. The increased propensity to adatom diffusion is in line with incomplete surface melting just below the melting temperature.[30] In the indirect mechanism [Fig. 2(a)] it is assumed that either one or both adatoms delocalize and move toward the other and exchange their positions either at the opposite T_4 position (mechanism i) or in between the two T_4 positions (mechanism ii). It is indeed fairly easy to destabilize both types of adatoms by the tip. From the geometry of the Ge(111)-$c(2\times8)$ surface in Fig. 1 it is seen that only the rest atoms and adatoms can easily by affected by the tip. We found that adatom manipulation has little effect on the stability of the nearby adatoms, and it is the rest atom manipulation that has destabilizing effect on the adatoms. The adatoms on (111) semiconductor surfaces such as Si or Ge are stabilized by charge transfer from adatoms to rest atoms.[31] Logically, reversal of the adatom $\rightarrow$rest atom charge transfer will destabilize the adatoms from their equilibrium T_4 positions. The charge-transfer blocking/reversal can be achieved by approaching a reactive tip apex to the rest atom dangling bond whereby a bond will be formed. This simple idea was tested both by a series of static calculations as well as by a finite-temperature MD simulations (see Fig. 3). In both cases both adatoms (Ge and Sn) were found to easily delocalize from their T_4 positions. If the process is thermally activated, the ability to exchange the (Sn, Ge)-pairs in different directions is striking, as adatom

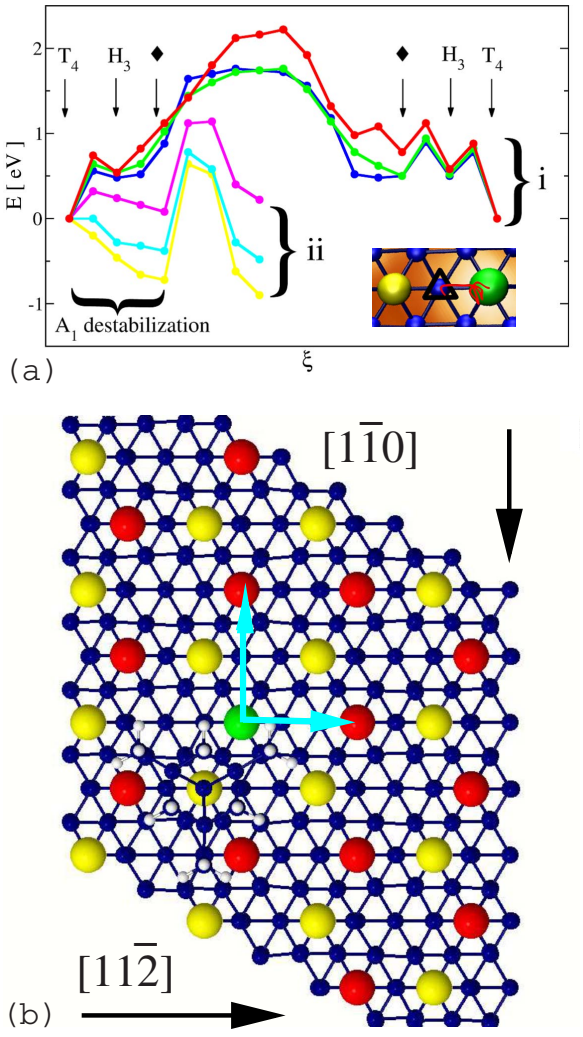

FIG. 3. (Color online) Static energy profiles for the indirect process of (Sn, Ge)-pair exchange between two T_4 sites in $[1\bar{1}0]$ direction labeled by ξ. The PESs were computed with a 10 atom Ge tip (Ref. 9) positioned over a rest atom as shown in the lower panel. The light blue arrow indicates the line along which the PES was computed in the $[1\bar{1}0]$ direction. Process (i): Sn diffusion toward and exchange around a Ge adatom in a T_4 position (red: no tip; green: tip in equilibrium over a rest atom; blue: tip over rest atom in a 0.5 Å compression; and magenta: tip over rest atom in 1.0 Å compression). Process (ii): exchange around a ♦ site, with Sn adatom staring the diffusion (magenta: tip over rest atom in a 1.0 Å compression; cyan: tip over rest atom in a 1.25 Å compression; and orange: tip over rest atom in a 1.25 Å compression but with the Ge atom diffusing first to the ♦ site). For more details see text and Ref. 21. Finite-temperature delocalization of Sn adatom is shown in the inset by projection of MD trajectory onto the surface plane (red trace). The simulation was done at 1800 K with a 10 atom Ge tip (Ref. 9) indenting a nearby rest atom by 1.25 Å; see the lower panel. Color coding of atoms follows Fig. 1.

diffusion was found to be very anisotropic, with $[1\bar{1}0]$ being the "easy" direction and the $[11\bar{2}]$ the "hard" direction for diffusion.[32] As shown in Fig. 4 the diffusion barriers into empty T_4 sites in both directions are almost equal (0.6–0.8 eV), with no hard and easy diffusion directions.[32] However, static energy calculations in Fig. 3 show that interchange of delocalized atom(s) cost an inordinate amount of energy (1–2 eV) depending on the details of the mechanism considered. Hence, at finite temperatures the adatoms destabilized by the tip will be bouncing back and forth from their T_4 positions without causing the experimentally observed (Ge, Sn)-pair exchange.[8]

How can the pairwise exchange proceed? On energy grounds, the destabilized adatom "diffusion" into the adjacent T_4 site can only proceed into a vacant site. This is shown in Fig. 4 which demonstrates the huge reduction in the dominant first diffusion barrier from 0.55 eV (0.65 eV) to 0.28 eV (0.15 eV) along $[1\bar{1}0]$ ($[11\bar{2}]$) direction upon indenting the nearest rest atom by a tip (see Fig. 4). However, the successive barriers are seen to be affected much less. For example, the barrier between the H_3 and ♦ sites in the $[1\bar{1}0]$ direction only reduces from 0.5 to 0.38 eV if the tip is positioned as shown in Fig. 3, i.e., over a rest atom close to the initial T_4 site. By moving the tip to the next rest atom in the $[1\bar{1}0]$ direction, the second barrier reduces further to just 0.28 eV, i.e., to the same tip-reduced height found for the first barrier. Similar results are found also for the other barriers and the $[11\bar{2}]$ direction. Hence, moving the tip and indenting the rest atoms along the diffusion pathways leads to reduction in the successive barriers and makes the adatoms move along with the tip into an empty T_4 site. The natural explanation is along the direct process [Fig. 2(b)]. As the energy of an oscillating tip is many orders of magnitude larger than any barrier encountered in removing one of the adatoms blocking the diffusion, we assume that the process will consist of three major steps: (i) creation of an adatom

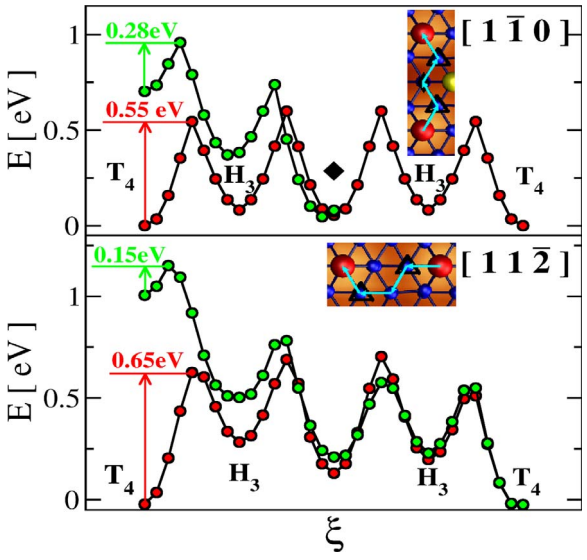

FIG. 4. (Color online) PESs for Sn adatom diffusion toward a nearby empty T_4 site without the presence of a tip (red) and with tip indenting the rest atom closest to the Sn adatom by 1.25 Å (green). Adatom diffusion in the $[1\bar{1}0]$ direction (top) and in the $[11\bar{2}]$ direction (bottom). Both profiles were computed for geometries and tip position shown in the lower panel of Fig. 3. The diffusion paths are shown in the insets. The green/red numbers indicate the dominant barrier reduction upon rest atom indentation.

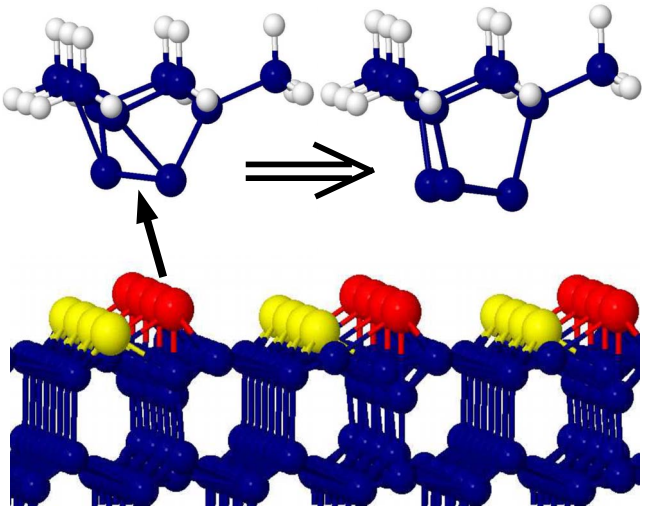

FIG. 5. (Color online) Schematics of a spontaneous formation of a trimerized apex from a dimer-terminated tip (Ref. 28). Color coding of atoms follows Fig. 1.

vacancy by a pick-up process by a tip; (ii) the broken symmetry will make the almost barrierless tip-assisted diffusion from an occupied T_4 site into an adjacent empty T_4 site possible, see Figs. 2 and 4; (iii) deposition of a tip-bonded adatom back onto the surface and diffusion into the vacancy previously formed by the adatom pick-up process. While step (ii) follows from Fig. 4, the ability of the tip to perform the adatom pick-up/deposition processes without causing observable differences in the experimental signal due to apex changes remains to be demonstrated.

In line with experimental results,[8] we have found that the pick-up/deposition processes are only possible with certain model tip apexes. For example, we were unable to perform the pick-up/deposition processes with the 10 atom Ge tip,[9] the dimerized tip,[28] etc. However, the dimerized tip, which was found to be consistent with experimental results in the imaging mode,[28] spontaneously formed trimerized tip apex by removing an adatom from the surface (see Fig. 5) upon close approach to the Ge adatom. The trimerized apex is unique as it is barely reactive when further away from the surface. On close approach to the surface the Ge triangle at the apex opens up, forming two highly reactive ends able to bind and manipulate the adatoms.

As shown in Fig. 6, the model trimerized tip has the adatom pick-up/deposition ability. When close to the occupied target T_4 site, the first oscillation with the trimerized terminated tip causes adatom pickup, while the successive oscillations retain the manipulation result unchanged. Similarly, approaching a vacant T_4 site by a trimerized terminated tip with an adatom temporarily bonded to it causes adatom deposition onto the surface, a result which the successive oscillations do not revert. One might wonder why the adatom is left on the surfaces without being picked up again. We note that in the case of deposition, the adatom is not returned to the T_4 site but rather remains trapped in the diffusion channel(s) from which it is delocalized and moved by the tip as explained above. This demonstrates that the manipulation process is irreversible with respect to the successive tip oscillations. Figure 6 shows that the processes are not only irreversible but also that the apex modification will not be experimentally noticeable. As can be seen, the differences in PESs before and after manipulation are tiny and will be masked by a number of discontinuities arising due to the other tip/substrate processes (see Fig. 6) and in real experiments also by finite-temperature and associated electronics effects.[24]

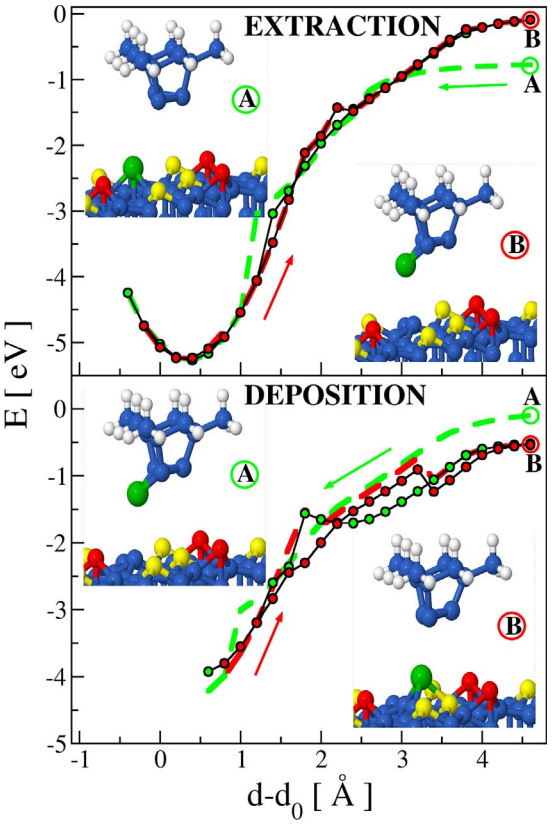

FIG. 6. (Color online) PESs for adatom extraction (top) and adatom deposition (bottom) with a trimerized apex. Dashed line: first oscillation of the tip, and black line with dots: second/successive tip oscillations. Green: tip approach; red: tip retraction. The insets show the configurations at the (a) beginning of the process and (b) end of the process. $d-d_0$ is the tip-surface distance (Ref. 9). Color coding of atoms follows Fig. 1.

In summary, we presented an *ab initio* simulation of the experimentally realized NC AFM manipulation of the (Sn, Ge)-pair exchange on the Ge(111)-$c(2\times8)$ surface. Using simple models for the basic steps of the intricate manipulation process we show that the experimental results are compatible only with the "direct process" which involves simultaneous occurrence of tip-induced pick-up/deposition and diffusion processes of the adatoms on the surface. The pick-up/deposition processes were so far not considered as the accompanying apex modification was expected to generate a significant change in the measured signal. The computed energy-distance curves demonstrate that for certain model tip apexes these processes are not only irreversible but also undetectable experimentally. Similar line of arguments applies equally to the lateral manipulation of the Ge adatoms on the Ge(111)-$c(2\times8)$ surface.[7,33]

The authors gratefully acknowledge financial support by APVV under Contract No. APVT-20-021504, and O. Custance and N. Oyabu, Osaka, Japan, for fruitful discussions and for providing us with the experimental results.

---

*Author to whom correspondence should be addressed; ivan.stich@savba.sk

[1] S. Morita, R. Wiesendanger, and E. Meyer, *Noncontact Atomic Force Microscopy* (Springer, Berlin, 2002).
[2] R. García and R. Pérez, Surf. Sci. Rep. **47**, 197 (2002).
[3] F. J. Giessibl, Rev. Mod. Phys. **75**, 949 (2003).
[4] M. A. Lantz *et al.*, Science **291**, 2580 (2001).
[5] Y. Sugimoto *et al.*, Nature (London) **446**, 64 (2007).
[6] N. Oyabu, O. Custance, I. Yi, Y. Sugawara, and S. Morita, Phys. Rev. Lett. **90**, 176102 (2003).
[7] N. Oyabu *et al.*, Nanotechnology **16**, S112 (2005).
[8] Y. Sugimoto *et al.*, Nat. Mater. **4**, 156 (2005).
[9] R. Pérez, M. C. Payne, I. Štich, and K. Terakura, Phys. Rev. Lett. **78**, 678 (1997); R. Pérez, I. Štich, M. C. Payne, and K. Terakura, Phys. Rev. B **58**, 10835 (1998).
[10] J. Tobik, I. Štich, and K. Terakura, Phys. Rev. B **63**, 245324 (2001); S. H. Ke, T. Uda, I. Stich, and K. Terakura, *ibid.* **63**, 245323 (2001).
[11] P. Dieška, I. Štich, and R. Pérez, Phys. Rev. Lett. **91**, 216401 (2003).
[12] A. I. Livshits, A. L. Shluger, A. L. Rohl, and A. S. Foster, Phys. Rev. B **59**, 2436 (1999).
[13] T. Trevethan *et al.*, Nanotechnology **18**, 345503 (2007); **17**, 5866 (2006).
[14] M. B. Watkins and A. L. Shluger, Phys. Rev. B **73**, 245435 (2006).
[15] S. Hirth, F. Ostendorf, and H. Reichling, Nanotechnology **17**, S148 (2006).
[16] See, for instance, D. M. Eigler and E. K. Schweizer, Nature (London) **344**, 524 (1990); D. M. Eigler, C. P. Lutz, and W. E. Rudge, *ibid.* **352**, 600 (1991); L. Bartels, G. Meyer, and K.-H. Rieder, Phys. Rev. Lett. **79**, 697 (1997); G. Dujardin, A. Mayne, O. Robert, F. Rose, C. Joachim, and H. Tang, *ibid.* **80**, 3085 (1998).
[17] See, for instance, T. A. Jung *et al.*, Science **271**, 181 (1996); B. C. Stipe, M. A. Rezaei, and W. Ho, *ibid.* **279**, 1907 (1998).
[18] See, for instance, B. C. Stipe, M. A. Rezaei, and W. Ho, Phys. Rev. Lett. **79**, 4397 (1997); H. J. Lee and W. Ho, Science **286**, 1719 (1999); J. R. Hahn and W. Ho, Phys. Rev. Lett. **87**, 166102 (2001).
[19] P. Dieška, I. Štich, and R. Pérez, Phys. Rev. Lett. **95**, 126103 (2005).
[20] Y. Sugimoto, P. Jelinek, P. Pou, M. Abe, S. Morita, R. Perez, and O. Custance, Phys. Rev. Lett. **98**, 106104 (2007).
[21] P. Dieška and I. Štich, Nanotechnology **18**, 084016 (2007).
[22] N. Oyabu *et al.*, Contribution at Eight International Conference on Noncontact Atomic Force Microscopy, Bad Essen, Germany, August 2005.
[23] O. Custance and N. Oyabu, private communication.
[24] J. Polesel-Maris and S. Gauthier, J. Appl. Phys. **97**, 044902 (2005); T. Trevethan, M. Watkins, L. N. Kantorovich, and A. L. Shluger, Phys. Rev. Lett. **98**, 028101 (2007).
[25] D. Marx and J. Hutter, in *Modern Methods and Algorithms of Quantum Chemistry*, edited by J. Grotendorst (NIC, FZ Jülich, 2000), p. 301; for downloads see www.theochem.ruhr-uni-bochum.de/go/cprev.html
[26] S. Goedecker, M. Teter, and J. Hutter, Phys. Rev. B **54**, 1703 (1996); C. Hartwigsen, S. Goedecker, and J. Hutter, *ibid.* **58**, 3641 (1998).
[27] J. P. Perdew, K. Burke, and M. Ernzerhof, Phys. Rev. Lett. **77**, 3865 (1996); Phys. Rev. Lett. **78**, 1396 (1997); **80**, 891 (1998).
[28] N. Oyabu, P. Pou, Y. Sugimoto, P. Jelinek, M. Abe, S. Morita, R. Perez, and O. Custance, Phys. Rev. Lett. **96**, 106101 (2006).
[29] G. Henkelman, B. P. Uberuaga, and H. Jónsson, J. Chem. Phys. **113**, 9901 (2000); G. Henkelman and H. Jónsson, *ibid.* **113**, 9978 (2000).
[30] N. Takeuchi, A. Selloni, and E. Tosatti, Phys. Rev. Lett. **72**, 2227 (1994).
[31] See, for instance, I. Štich, M. C. Payne, R. D. King-Smith, J. S. Lin, and L. J. Clarke, Phys. Rev. Lett. **68**, 1351 (1992).
[32] N. Takeuchi, A. Selloni, and E. Tosatti, Phys. Rev B **49**, 10757 (1994).
[33] P. Dieška and I. Štich (unpublished).